Optical spin orientation in strained Ge/SiGe quantum wells: A tight-binding approach

Michele Virgilio and Giuseppe Grosso

NEST-INFM and Dipartimento di Fisica "E. Fermi," Università di Pisa, Largo Pontecorvo 3, I-56127 Pisa, Italy

(Received 14 July 2009; revised manuscript received 19 October 2009; published 11 November 2009)

We present a theoretical investigation of electron-spin optical orientation in strained Ge/SiGe quantum wells. The atomistic $sp^3d^5s^*$ nearest-neighbor tight-binding model adopted, allows us to obtain the spin polarization of the excited electrons, as a function of frequency and direction of the incident radiation, in the presence of external fields, different strain conditions, and taking into account contributions arising from states out of the Brillouin zone center. Orbital projected densities of states further highlight spin mixing of the localized spin-orbitals composing the states involved in the optical transitions. Our results illustrate the potential of the adopted method as a theoretical tool to support experiments on optical manipulation of spins in group IV based heterostructures.

I. INTRODUCTION

Generation and detection of spin-polarized carriers in a semiconductor is of central importance for the study of spintronics and spin-optoelectronics phenomena.[1,2] Efficient generation of spin-polarized electrons can be realized by injection of polarized electrons from a magnetic material into the conduction band of a semiconductor[3,4] or by optical orientation of electrons excited from the valence band into the conduction band with circularly polarized light.[1,5] On the other side one can exploit the degree of circular polarization, P_{circ}, of the luminescence accompanying electron-hole recombination in a semiconductor to deduce the spin polarization along a given direction, P_s, of the injected carriers.[4,6]

Investigation of the polarization of interband optical transitions has been a traditional spectroscopic tool to gain information on the symmetry of electrons, holes and excitons in bulk semiconductors.[7,8] Moreover circular polarization of near gap time resolved spectroscopy luminescence has provided information on spin-relaxation mechanisms and contributed to highlight the difference between relaxation times in quantum wells (QWs) and bulk semiconductors.[9–11] Recently, the possibility that optically polarized electrons can emit terahertz radiation,[12] switch the intensity and polarization of a laser,[13] or reduce its threshold current,[14] has contributed to grow the interest on optical orientation in semiconductor systems.

Most of the work in this field has been theoretically addressed within the $\vec{k} \cdot \vec{p}$ multiband approach and has been concentrated on III-V based systems. However, understanding and control of spin polarization in group IV based structures is becoming a formidable challenge[15–19] toward the development of silicon integrable spintronic devices.[20] Electric injection of spin-polarized carriers in Si based systems has been first measured in Refs. 15 and 16 and optical spin orientation and polarized luminescence of Silicon has been theoretically investigated in Ref. 21. To our knowledge, until present, no study on optical orientation in Ge-rich structures has been reported, despite a number of recent articles indicate Germanium as most promising material in the run to Si-integrable photonics.[22–29]

Germanium is an indirect gap material, with the minimum of the conduction band at the L point, only 134 meV lower in energy than the minimum at the Γ point. For Ge-based heterostructures strong confinement of Γ electrons in Ge-rich SiGe QW systems has been unambiguously demonstrated and already exploited to design efficient electro-optical modulators relying on the quantum confined stark effect;[23,24] conversely the experimental demonstration of significant conduction confinement potential in low-Ge content QWs is still lacking. More exciting, Sun *et al.*[25] recently observed for the first time direct band-gap electroluminescence at room temperature from strained Ge/Si heterojunction light-emitting diodes, paving the way to electrically pumped light emitters integrated on Si with Germanium as active material. Adding the spin degree of freedom to the advances in Ge-rich heterostructures mentioned above could largely increase their impact in future technology.

In this paper, we investigate numerically, by a tight-binding (TB) model, optical orientation of quantum confined carriers in the conduction band of strained [001]-Ge QWs, embraced by SiGe barriers. In particular, we study the initial degree of spin polarization P_s for electrons photocreated soon after the optical absorption across the QW direct gap by a pulsed quasimonochromatic circularly polarized radiation.

The physics of optical orientation by circularly polarized light relies on the symmetries of the near gap valence and conduction states at the Γ point. The orbital contributions to the heavy hole (HH), light hole (LH), split-off (SO) valence states, and to the lowest conduction state at Γ are essentially identical in III-V compounds and group IV elements and then the same selection rules hold for the involved optical transitions occurring at $\vec{k}_\parallel = 0$. As sketched in Fig. 1, the absorption of left (σ^+) and right (σ^-) polarized radiation, must preserve the (total) magnetic quantum number. It follows that, choosing the quantization axis along the $\hat{z}$ direction only transitions indicated by arrows are allowed if the circularly polarized radiation propagates in the same direction.[1] Defining the spin polarization as $P_s = \frac{N_+ - N_-}{N_+ + N_-}$ where $N_+(N_-)$ is the number of electrons with spin up (down), and considering that the relative strength of the HH$\rightarrow c\Gamma$ and LH$\rightarrow c\Gamma$ transitions at Γ is 3, one gets that in bulk semiconductors for σ^+ radiation resonant with the HH,LH$\rightarrow c\Gamma$ degenerate energies, P_s is equal to -0.5.[1] On the other hand, if the heavy hole, light hole degeneracy is removed by strain or quantum
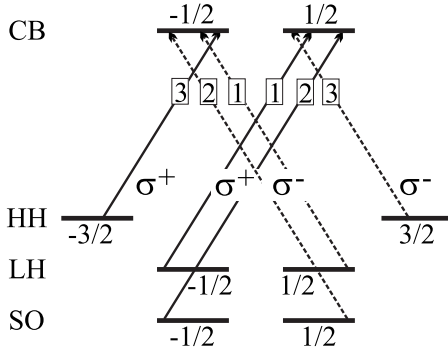
FIG. 1. Schematic of the zone center highest valence and lowest conduction energy levels for the compressively strained Ge QW system discussed in the text. Magnetic quantum numbers m refer to the component along the growth direction of the total angular momentum J of the heavy, light, and split-off states and of the lowest Γ conduction state. Dipole allowed transitions for left (σ^+) and right (σ^-) circularly polarized radiation, incident normally to the QW plane, are indicated by arrows. Solid (dashed) lines refer to $\sigma^+(\sigma^-)$ photons whose J_z angular momentum is equal to $+1(-1)$. The numbers enclosed in squares indicate the relative strength of the allowed transitions.

confinement as in Fig. 1, for excitation energy at the absorption edge, P_s can in principle reach the limit value of -1 (see Refs. 10 and 30).

However, the schematic Fig. 1 represents a quite crude model where different and potentially relevant effects are neglected. In fact the description of valence states in terms of pure $|J,J_z\rangle$ states strictly holds at the Gamma point. Therefore mixing of $|J,J_z\rangle$ states has to be taken into account to describe optical excitations related to states with nonvanishing momentum which contribute to the near gap direct absorption. Moreover, if a strain field is present as usually happens in SiGe heterostructures, it further contributes to reduce the symmetry and to mix $|J,J_z\rangle$ states, also at the Γ point. Finally, if an external electric field is applied in the active region, as may be the case for device applications, the twofold degeneracy of the levels with $\vec{k}_\parallel \neq 0$ is lifted due to the inversion asymmetry induced by the field and band mixing further increases.[31]

To take into account the above-mentioned effects a more realistic study of P_s requires a numerical approach. To this aim we have adopted a $sp^3d^5s^*$ tight-binding model which has already provided very accurate descriptions of electronic and optical properties of SiGe multilayer systems (see for instance Refs. 24 and 32 and references therein). Our tight-binding model includes spin-orbit coupling, guarantees an accurate evaluation of the orbital contributions of the states trough the whole Brillouin zone and allows to properly consider effects of strain, external fields, alloying, and heterointerface potential alignment. Moreover optical transitions and excitonic contributions are evaluated with the same formalism.[33]

We investigate the initial degree of the spin polarization in Ge/SiGe QW systems resulting from the optical absorption across the direct gap of pulsed quasimonochromatic circular polarized radiation. P_s is studied as a function of the near gap excitation energy and contributions arising from different va-

lence subbands are identified and discussed. Moreover we describe the variation in P_s induced by electric fields or by external strain fields applied along the growth direction. Finally, results on the dependence of P_s on the angle of the incident radiation field are presented. Details on the model are given in Sec. II; numerical results are presented and discussed in Sec. III; Sec. IV contains our conclusions.

II. SYSTEM DESCRIPTION AND NUMERICAL MODEL

The systems investigated in this paper are composed of compressively strained 48 monolayers Ge QWs, embraced by tensile strained $Si_{0.2}Ge_{0.8}$ barriers, lattice matched to relaxed $[001]$-$Si_{0.1}Ge_{0.9}$ substrates. To obtain the electronic structure of these systems, we start evaluating the equilibrium positions of the ions by means of elasticity theory,[34] as discussed in Ref. 35. In our atomistic description heterointerfaces are assumed sharp and the barrier thickness is chosen so to ensure that the wave functions for the confined QW states are extinguished well before the boundaries of the well+barriers system. With this choice periodic or hard wall boundary conditions along the $[001]$ direction can be equivalently adopted, while in the growth plane periodic boundary conditions are assumed.

The electronic states are described by means of a first neighbors $sp^3d^5s^*$ TB Hamiltonian which includes spin-orbit interaction. We adopt self and hopping energy parameters derived by Jancu *et al.*[36] for relaxed bulk silicon and germanium crystals. Since Si and Ge are miscible in the whole composition range, alloying in the barriers is treated within the virtual crystal approximation (VCA), i.e., with linear interpolation, with Ge concentration, of the parameters of Ref. 36. A recent discussion of such approximation in the TB framework can be found in Ref. 37. The modifications of the electronic structure due to the strain field present in the barrier and well regions are included in the model by suitable scaling laws for the hopping parameters.[36] The band alignment along the growth direction due to the strained Ge/$Si_{0.2}Ge_{0.8}$ interfaces, is inserted in the model adding a constant term to the site diagonal energy parameters of the Hamiltonian in the barrier region. Following Rieger and Vogl,[38] this term is obtained interpolating linearly with the Ge concentration the values calculated by Van de Walle and Martin for the discontinuity under different strain conditions of the HH, LH, and spin-orbit (SO) barycenter at the pristine $[001]$-Si/Ge interface.[34] As well, uniform electric fields superimposed along the growth direction are modeled by means of on-site z-dependent contributions to the Hamiltonian.

For the strained well material (Ge) the bottom of the conduction band is located at the L point. With respect to this energy level, the L point conduction state in the barrier ($Si_{0.2}Ge_{0.8}$) is 111 meV higher in energy; the conduction-band edge at the Γ point for the well and barrier are found 183 and 581 meV higher in energy, respectively. In agreement with similar results reported in the literature,[24] the obtained band edges alignment indicates robust confinement in the Ge region of both L and Γ electrons; the fundamental gap of the QW system remains indirect. In the valence we find
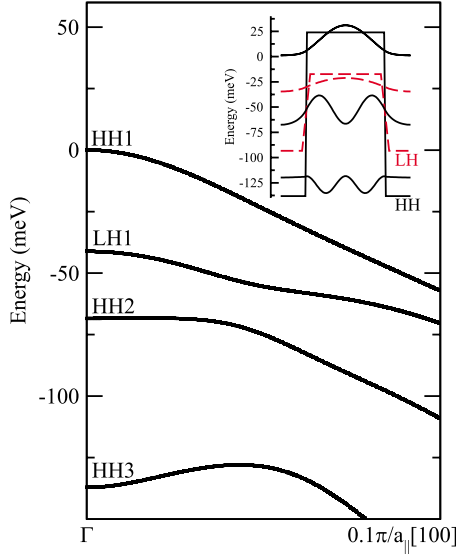
FIG. 2. (Color online) Near gap valence-band structure for the compressively strained [001]-Ge/Si$_{0.2}$Ge$_{0.8}$ QW system discussed in the text. Results are reported for a small part of the Γ-$X_\parallel$ segment of the Brillouin zone. The labels indicate subbands corresponding to the heavy and light hole QW states. In the inset the HH (solid line) and LH (dashed line) band profiles are shown together with the square modulus of the confined wave functions.

for the HH and LH band discontinuities at the Ge/Si$_{0.2}$Ge$_{0.8}$ interface the values of 162 and 75 meV, respectively. The energy separation between the HH and LH bands of the strained Ge layer is about 41 meV (see inset in Fig. 2). From the diagonalization of the system Hamiltonian we find that three heavy hole QW states (HH1, HH2, and HH3) are confined in the Ge region, while, due to the less robust LH offset, only one light hole state (LH1) is fully confined in the Ge well. LH2, LH3, and SO1 states lie at lower energies, resonant with continuum valence states. The near gap subband energies sequence in the valence band is shown in Fig. 2.

It is worth to notice that the different values for the valence-band offsets at the strained Si$_{1-x}$Ge$_x$/Si$_{1-y}$Ge$_y$ interfaces reported in the literature suggest that an indetermination of the order of 10 meV can be assumed for them. We have thus verified that, varying the offsets within this range of uncertainty, the near gap energy levels do not change significantly, resulting in almost unchanged polarization spectra.

Single particle absorption across the direct gap for $\sigma^\pm$ polarized light incident normally to the QW plane is calculated according to the expression

$$
\begin{aligned}
\alpha(\hbar\omega) &= \sum_{c,v} \alpha_{c,v}(\hbar\omega) \\
&= \sum_{c,v} \frac{2\pi e^2 \hbar}{n_0 c m_0 V \Gamma} \\
&\times \sum_{\vec{k}} \frac{P_{c,v}^\epsilon(\vec{k})}{E_c(\vec{k}) - E_v(\vec{k})} \cdot \frac{1}{1 + \left(\dfrac{E_c - E_v - \hbar\omega}{\Gamma}\right)^2},
\end{aligned} \quad (1)
$$

where $P_{c,v}^\epsilon(\vec{k}) = (2/m_0)|\langle c,\vec{k}|\hat{\epsilon}\cdot\vec{p}|v,\vec{k}\rangle|^2$ is the squared modulus of the dipole matrix element, expressed in eV, between conduction $|c,\vec{k}\rangle$ and valence $|v,\vec{k}\rangle$ states with energies E_c and E_v, respectively, and $\hat{\epsilon}$ is the vector which correspond to the $\sigma^\pm$ polarizations. The volume V is equal to the product of the unit area in the QW plane and the width of the Ge plus barrier region; n_0 is the QW refractive index and it is almost independent on the frequency in the energy range of interest. Its value has been chosen equal to the static bulk Germanium refractive index. A Lorentzian distribution is introduced in Eq. (1) to phenomenologically take into account linewidth effects, and we set $\Gamma = 5$ meV, as suggested by the low-temperature absorption measurements reported in Ref. 24. Since in the semiempirical tight-binding framework the wave functions of the localized basis orbitals are not know, dipole matrix elements $|\langle c,\vec{k}| \hat{\epsilon}\cdot\vec{p}|v,\vec{k}\rangle|$ have been calculated exploiting the tight-binding hopping parameters as outlined in Ref. 33.

For each couple of bands (c,v) involved in expression (1), excitonic contributions have been evaluated by means of the two-dimensional (2D)-Elliott expression[39]

$$
\begin{aligned}
\alpha_{c,v}^{ex}(\hbar\omega) = \alpha_{c,v}(\hbar\omega) &\left[\sum_{n=0}^{\infty} \frac{4}{\left(n+\frac{1}{2}\right)^3} \delta\left(\Delta + \frac{1}{\left(n+\frac{1}{2}\right)^2}\right) \right. \\
&\left. + \Theta(\Delta) \frac{e^{\pi/\sqrt{\Delta}}}{\cosh\left(\dfrac{\pi}{\sqrt{\Delta}}\right)} \right],
\end{aligned} \quad (2)
$$

where $\alpha_{c,v}(\hbar\omega)$ is given in expression (1), $\Delta = \frac{\hbar\omega - E_{c,v}}{E_0}$, $E_{c,v}$ is the energy difference of the considered couple of bands at the band edge, and $4E_0$ is the exciton binding energy. The two terms in the square brackets in Eq. (2) account for the below (Rydberg-like) and above (Coulomb enhancement) gap features. Also for the Rydberg states, a lineshape Lorentzian broadening with the same full width at half maximum (FWHM) substitutes the δ function in the numerical calculations. For the Γ point excitonic binding energy we have adopted the value $4E_0 = 3.6$ meV, in agreement with the theoretical results for Ge/SiGe finite QWs reported in Refs. 40–42.

The electronic spin polarization spectrum $P_s(\hbar\omega)$ is given by

$$
P_s(\hbar\omega) = \frac{\displaystyle\sum_{c,v}\sum_{\vec{k}} P_{c,v}^\epsilon(\vec{k}) S(\vec{k}) \cdot \frac{1}{1 + \left(\dfrac{E_c - E_v - \hbar\omega}{\Gamma}\right)^2}}{\displaystyle\sum_{c,v}\sum_{\vec{k}} P_{c,v}^\epsilon(\vec{k}) \cdot \frac{1}{1 + \left(\dfrac{E_c - E_v - \hbar\omega}{\Gamma}\right)^2}}, \quad (3)
$$

where again Γ is set equal to 5 meV and $S(\vec{k}) = \langle c,\vec{k}|S_z|c,\vec{k}\rangle$ is the expectation value of the z component of the spin operator, evaluated for the conduction state involved in the $|v,\vec{k}\rangle \rightarrow |c,\vec{k}\rangle$ transition. We note that in the above expression the HH-LH coupling of the hole states at nonvanishing mo-

mentum, the k dependence of the dipole matrix element, and the mixing of $|\uparrow\rangle$ and $|\downarrow\rangle$ electronic spin states, are properly taken into account. In particular, as discussed in the following, spin states mixing effect is crucial for the description of optical orientation under applied electric fields. To include in expression (3) also excitonic effects, we have corrected the contribution to the polarization of each couple of valence and conduction bands by means of the 2D-Elliott formula as already performed for optical absorption in Eq. (2).

As a final remark we stress that the $P_s(\hbar\omega)$ spectrum given by Eq. (3) describes the initial degree of spin polarization as a function of the pulsed excitation energy, i.e., immediately after promotion of carriers in the conduction band and before any intra or interband relaxation process takes place. As mentioned in the introduction, the initial degree of optical spin polarization can be measured optically investigating the degree of circular polarization of the photoluminescence light. This kind of measurements have been mainly performed on III-V direct gap systems (see for instance Ref. 10). Usually it is assumed that the spin state is preserved during the momentum (intraband) relaxation in the conduction band which occurs before radiative recombination. Under the further hypothesis that holes in the valence are depolarized due to their faster spin-relaxation mechanisms or p doping, the degree of circular polarization from the luminescence allows a direct measure of the spin orientation. In the case of SiGe structures like the ones investigated in this paper, we notice that one should consider that excited spin-polarized electrons at Γ can scatter also into the L minima before radiative recombination takes place. This may complicate the analysis of the luminescence light as discussed in Ref. 21.

III. NUMERICAL RESULTS

The electronic spin-polarization spectrum, calculated for excitation energies $\hbar\omega$ above the direct gap absorption threshold, and with σ^- polarized light incident normally to the QW plane, is shown in Fig. 3(a). For comparison, the corresponding absorption spectrum is reported in Fig. 3(b). To better evidence the role of excitonic effects in the optical orientation process, calculations have been performed both with (solid lines) and without (dot-dashed lines) the inclusion of the excitonic contribution. As indicated by the vertical labels in Fig. 3(a), the main features of the polarization spectrum can be associated to the transitions involving the heavy, light, and split-off subbands in the valence and the $c\Gamma1$ and $c\Gamma2$ states in the conduction band (see also Fig. 2). In agreement with the scheme of Fig. 1, positive peak values for the spin polarization are found at the HH1-$c\Gamma1$ (1030 meV) and HH2-$c\Gamma2$ (1327 meV) resonances while polarization dips are related to the LH1-$c\Gamma1$, LH3-$c\Gamma1$, and SO-$c\Gamma1$ transitions. In particular, polarized light at the HH1-$c\Gamma1$ energy gives the absolute maximum of the polarization spectrum with $P_s \simeq 0.96$. This high value for P_s indicates that optical spin polarization is quite robust against band mixing induced by the strain field in the Ge active region.

We notice that for the energy range shown in Fig. 3 the polarization spectrum is always positive and P_s is about
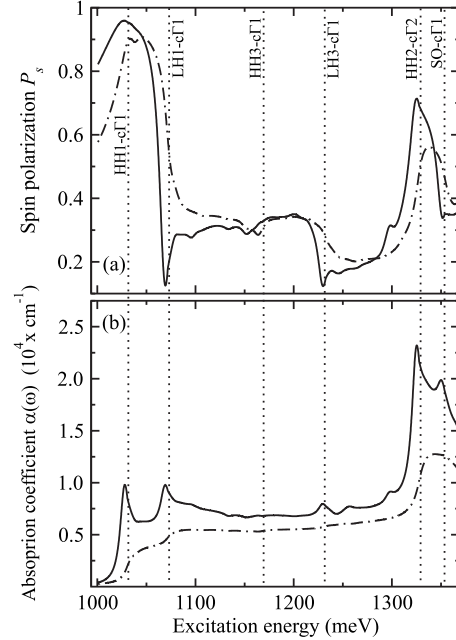
FIG. 3. Spin polarization P_s as a function of energy for the conduction electrons optically excited by right-circularly polarized light, incident normally to the QW plane (panel a). In panel (b) the corresponding absorption spectrum $\alpha(\hbar\omega)$ is reported. The threshold energies for the relevant interband transitions are indicated by vertical labels. Solid (dashed) curves have been obtained including (not including) excitonic contributions in the model.

0.125 at the LH1-$c\Gamma1$ threshold energy. At this energy both the HH1-$c\Gamma1$ and LH1-$c\Gamma1$ transitions are active and contribute with opposite signs to P_s. Therefore the resulting value depends on the relative intensity of their dipole matrix elements and the joint density of states. For instance similar calculations reported in Ref. 43 for a GaAs/GaAlAs QW system, at the LH1-$c\Gamma1$ threshold energy, give $P_s = -0.78$; negative polarizations for GaAs/GaAlAs QWs at the LH1-$c\Gamma1$ excitation energies have been also measured in Ref. 10. In these cases the negative value of P_s is related to the negative effective mass along the parallel direction of the LH1 states.[43] In fact the inverted curvature of the LH1 energy dispersion causes a large joint density of states for the LH1-$c\Gamma1$ transition as compared with the HH1-$c\Gamma1$ one. This fact compensates the weaker LH1-$c\Gamma1$ dipole matrix element and P_s becomes negative. In the present case P_s remains positive in agreement with the positive hole effective mass found for the LH1 state (see Fig. 2). As one can expect, P_s can also depend on the value of the FWHM adopted for the Lorentzian broadening. As already mentioned, absorption measurements reported in Ref. 24 indicate as a reasonable value $\Gamma = 5$ meV. However, when comparing with experimental measurements Γ can be regarded as a fitting parameter which is related also to the quality of the sample. We have performed simulations with different values of Γ, observing negative polarizations at the LH1-$c\Gamma1$ resonance when Γ is less than 3 meV.

The above results refer to a symmetric QW system. It is also interesting to investigate optical spin orientation in asymmetric QW structures. As often happens in device ap-
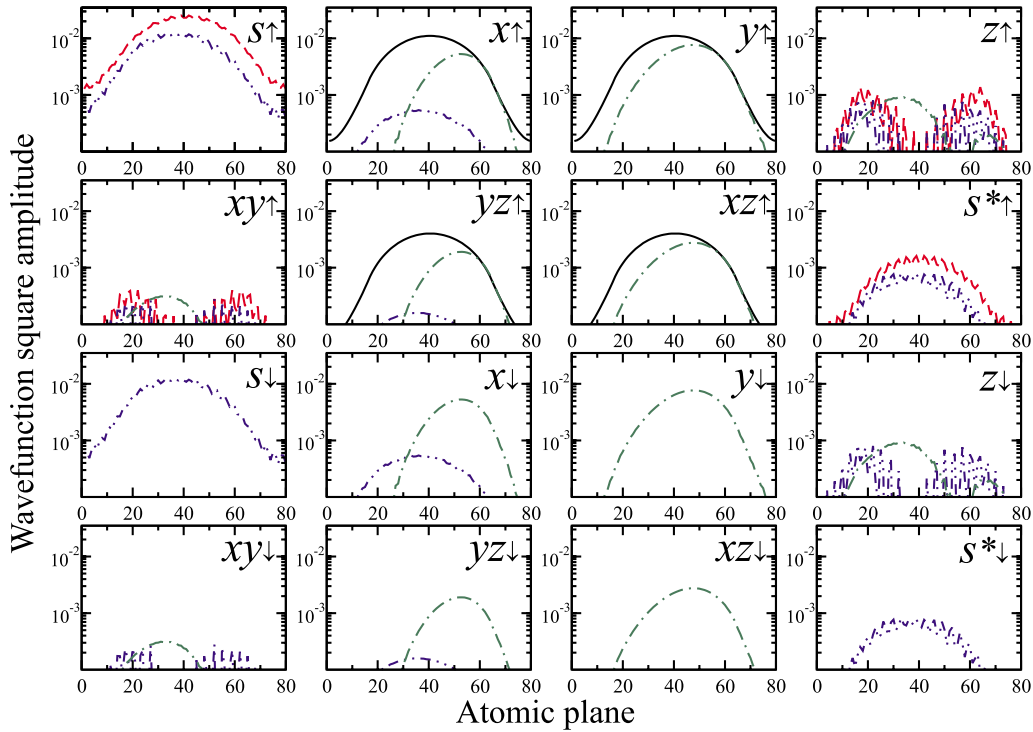
FIG. 4. (Color online) Orbital resolved wave functions for the $c\Gamma 1$ and HH1 states of the QW system discussed in the text. Red dashed (black solid) curve refers to the $c\Gamma 1$ (HH1) state, calculated at $k_\parallel=0$, in the absence of external electric fields. Blue dot-dot-dashed (green dot-dashed) curve refers to the $c\Gamma 1$ (HH1) state, calculated at $\vec{k}=(5\times 10^{-2},0,0)\pi/a_\parallel$ in the presence of an electric field of 3×10^{-4} mV/Å along the growth direction. Notice that in the two latter cases the wave functions involve both spin up and spin down orbital contributions. Orbital contributions to the $c\Gamma 1$ and HH1 states from $d_{3z^2-r^2}$ and $d_{x^2-y^2}$ orbitals are negligible and are not reported in the figure.

plications, asymmetry in QW systems is introduced, e.g., applying an electric bias along the growth direction. The electric-field influences optical orientation since, lowering the symmetry of the system, allows the presence of $k_\parallel$-linear spin-dependent terms in the effective electronic Hamiltonian. A recent discussion on the point-symmetry group of unbiased and biased [001] SiGe QW structures with finite barriers can be found in Ref. 44. The authors of Ref. 44 discuss structure, interface, and bulk inversion asymmetries and model their effect on the Δ electrons of Si/SiGe QW systems by means of a spin-dependent effective mass Hamiltonians within the envelope function approximation. The band mixing induced by the $k_\parallel$-linear spin-dependent terms influences the orbital contribution of the electronic levels near the Γ point and then it can deeply affect the optical orientation process.

The orbital analysis of the electronic states further helps to clarify the modifications induced by the electric field. As an example we shown in Fig. 4 the $c\Gamma 1$ (red dashed line) and HH1 (black solid line) states at the Γ point in the absence of electric fields. Their orbital components indicate that the considered states originate from the bulk $|S\uparrow\rangle$ and $\sqrt{1/2}|(X+iY)\uparrow\rangle$ states, respectively, (notice that with the adoption of the $sp^3d^5s^*$ basis set, also a contribution from the d and s^* orbitals with the same spin magnetic moment can be present in the wave function). For the chosen states each orbital contribution remains almost constant in a small segment along the [100] line of the reciprocal space (not shown). However, when an electric field is applied the analy-

sis of the states at $k_\parallel \neq 0$ indicates that, not only the envelope function barycenter shifts but, most important, also orbitals with $|\downarrow\rangle$ magnetic moment do contribute to the wave function (see blue dot-dot-dashed and green dot-dashed lines for $c\Gamma 1$ and HH1, respectively).

Our results for the dependence of the optical spin orientation on the electric field are summarized in Fig. 5 where the polarization spectrum is shown for different field strengths, ranging from $\mathcal{E}=0$ to $\mathcal{E}=7.5\times 10^{-4}$ mV/Å. In agreement with the above considerations, we observe a monotonic quenching of P_s as a function of the electric field $\mathcal{E}$. We notice that the quenching effect on the spin orientation for the HH1-$c\Gamma 1$ transition results to be relatively more efficient as compared to its action on the LH1-$c\Gamma 1$ transition. It follows that at the LH1-$c\Gamma 1$ energy and for the field strengths shown in Fig. 5, negative spin polarization is achieved. In the investigated range, an exponential fit for the maximum of the spin polarization peak related to the HH1-$c\Gamma 1$ absorption, $P_s^{\max}(\mathrm{HH1})$, well reproduces the numerical data (see inset in Fig. 5) with an extinction coefficient $\beta\simeq 3.0\cdot 10^3$ Å/mV.

We now briefly discuss the dependence of the optical spin orientation on the direction of the incident light. In Fig. 6 it is shown how the optical orientation along the growth axis (z) depends on the angle δ between the growth axis and the direction of the incident radiation. When δ varies from zero to $\frac{\pi}{2}$, every feature in the P_s spectrum is monotonically suppressed and, for $\delta=\frac{\pi}{2}$, the P_s spectrum vanishes identically. This behavior can be explained focusing for instance on the
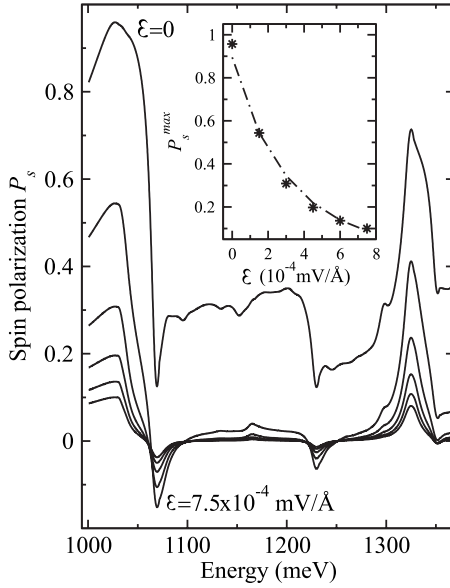
FIG. 5. Spin polarization P_s for electrons optically excited by right-circularly polarized light incident normally to the QW plane, calculated as a function of energy at different electric field strengths, ranging form zero to 7.5×10^{-4} mV/Å. The maximum degree of spin polarization $P_s^{\max}$ is achieved at energies close to the HH1 → $c\Gamma$1 transition and is reported in the inset as a function of the applied electric field. The dot-dashed curve represents an exponential fit.

FIG. 6. Spin polarization P_s for electrons optically excited by right-circularly polarized light, calculated at zero electric field for different incidence angles. δ=0 refers to light propagating along the growth direction; $\delta=\frac{\pi}{2}$ corresponds to light incident parallel to the QW plane. The maximum degree of spin polarization $P_s^{\max}$ is reported in the inset as a function of cos δ. The star and square symbols refer to the spin polarization at the HH1 → $c\Gamma$1 and LH1 → $c\Gamma$1 resonances, respectively. The dot-dashed (dotted) line is a quadratic (linear) fit. Notice that $P_s^{\max}$(LH1) is reported magnified by 4.

P_s peak at the HH1-$c\Gamma$1 resonance, whose magnitude, $P_s^{\max}$(HH1), is plotted as a function of cos δ in the inset of Fig. 6 (star symbols). For circularly polarized normal incident radiation, optical orientation occurs along the z direction and almost all electrons are in the $|\uparrow\rangle$ state. Analogously, for circularly polarized radiation incident along the y axis, i.e., parallel to the QW plane ($\delta=\frac{\pi}{2}$), the spin magnetic moment is optically oriented along the y axis. Since the expectation value of the S_z operator vanishes on spin states with the magnetic moment along the y axis, zero optical orientation along the z direction is obtained for parallel incident radiation (see Fig. 6). For $0 < \delta < \frac{\pi}{2}$, one can assume that almost all spins are aligned along the direction of the incident light. Expressing the corresponding spin state on the S_z basis set, we find that the $\langle S_z \rangle$ expectation value is a linear function of cos δ. However, at the HH1-$c\Gamma$1 resonance, a fit of the numerical results for the P_s maximum indicates $P_s^{\max}$(HH1) $\propto \cos \delta(2-\cos \delta)$ (see inset in Fig. 6). This nonlinear behavior of $P_s^{\max}$(HH1) as a function of cos δ is then not justified by the above argument. In fact, also the HH1-$c\Gamma$1 oscillator strength dependence on the angle of incidence as to be taken into account. Increasing the δ incidence angle, the magnitude of dipole matrix element for the HH1-$c\Gamma$1 decreases and, for parallel incident radiation, it becomes zero.[45] On the contrary the oscillator strength of the LH1-$c\Gamma$1 transition does not dependent on δ (see Ref. [45]); as a consequence the polarization peak $P_s^{\max}$(LH1) varies linearly with cos δ as shown in the inset of Fig. 6 (square symbols).

We conclude this section showing how an applied strain field influences the spin-polarization spectrum. To this aim we now choose infinite barriers for the QW. This allows us to focus on the modification of the states induced by the strain only in the active region, neglecting the dependence of the Ge/Si$_{1-x}$Ge$_x$ interface band alignment on the strain field. In Fig. 7 the P_s polarization spectrum is shown for different values of a [001]-biaxial strain field, ranging from $\epsilon_\parallel$=−3% to $\epsilon_\parallel$=4%. The strain field influences the orbital composition and relative energy position of the involved states. However, the main effect on the P_s spectrum is related to the modification of the energy distance among the valence states. Indeed we see from Fig. 7 that, increasing $\epsilon_\parallel$, the HH1-$c\Gamma$1 and LH1-$c\Gamma$1 transition energies redshift with different rates. As a consequence their energy distance decreases and the associated P_s peaks, which are related to opposite spin alignments, merge into the same energy region resulting in smaller values for P_s. This effect is more relevant in large QW systems. In fact, due to the smaller confinement energies, the energy distance between the HH1 and LH1 states in the case of tensile in-plane strain is further diminished, resulting in a stronger quenching; this is shown in Fig. 8 where we report the strain dependence of the P_s spectrum evaluated for a 80 monolayer Ge QW with infinite barriers.

IV. CONCLUSIONS

Using a $sp^3d^5s^*$ nearest-neighbor tight-binding model we have studied the initial spin polarization of electrons excited by circularly polarized radiation in the conduction band of strained Ge/SiGe quantum wells. We have shown that ab-
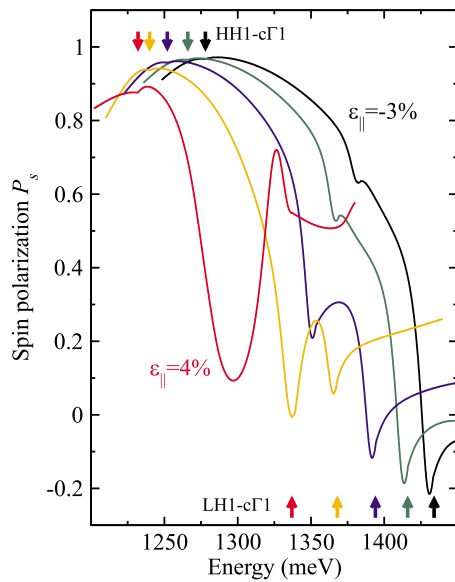
FIG. 7. (Color online) Spin polarization P_s for electrons optically excited by normal incident right-circularly polarized light, calculated at zero electric field for a 48 monolayer Ge QW with infinite barriers under different strain conditions. The considered in-plane strain field, ranges from $\epsilon_\parallel = -3\%$ to $\epsilon_\parallel = 4\%$. The corresponding HH1$\rightarrow c\Gamma$1 and LH1$\rightarrow c\Gamma$1 transition energies are indicated by arrows.

sorption coefficient of circularly polarized light can be put in close correspondence with the spin polarization of electrons in the conduction band. Moreover we have provided a picture of the spin polarization in terms of the states involved in the optical transitions and have shown how the polarization depends on the direction of the incident radiation, strain conditions, and external electric fields. The atomistic model adopted proves to be quite adequate for a quantitative description of the optical orientation of electron spins in the conduction band of strained semiconductor nanostructures.
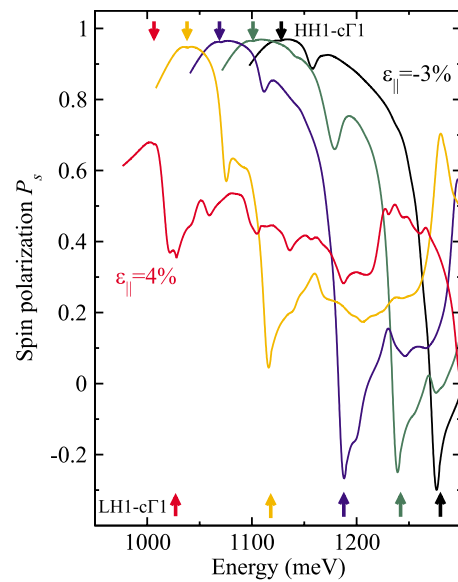
FIG. 8. (Color online) Same results as in Fig. 7 but in the case of an 80 monolayer Ge QW system.

We also stress that the tight-binding model here presented can be a precious support to experiments on optical manipulation of spins in the nanotechnology important group IV heterostructures, not only for spintronics in conventional devices, but also for quantum information processing that exploits the quantum coherence of the spins in the conduction band.

[1] I. Žutić, J. Fabian, and S. Das Sarma, Rev. Mod. Phys. **76**, 323 (2004).

[2] M. Oestreich *et al.*, Semicond. Sci. Technol. **17**, 285 (2002).

[3] H. Ohno, A. Shen, F. Matsukura, A. Oiwa, A. Endo, S. Katsumoto, and Y. Iye, Appl. Phys. Lett. **69**, 363 (1996).

[4] R. Fiederling, M. Keim, G. Reuscher, W. Ossau, G. Schmidt, A. Waag, and L. W. Molenkamp, Nature (London) **402**, 787 (1999).

[5] M. I. Dyakanov and V. I. Perel, *Optical Orientation* (Elsevier, Amsterdam, 1984), pp. 11–71.

[6] W. Wang, K. Allaart, and D. Lenstra, Phys. Rev. B **74**, 073201 (2006).

[7] *Optical Orientation*, edited by F. Meier and B. P. Zakharchenya (Elsevier, Amsterdam, 1984).

[8] Y. Kusrayev and G. Landwehr, eds., special issue on optical orientation, Semicond. Sci. Technol. **23** (2008).

[9] T. C. Damen, L. Vina, J. E. Cunningham, J. Shah, and L. J. Sham, Phys. Rev. Lett. **67**, 3432 (1991).

[10] S. Pfalz, R. Winkler, T. Nowitzki, D. Reuter, A. D. Wieck, D. Hägele, and M. Oestreich, Phys. Rev. B **71**, 165305 (2005).

[11] T. Uenoyama and L. J. Sham, Phys. Rev. B **42**, 7114 (1990).

[12] F. Nastos, R. W. Newson, J. Hübner, H. M. van Driel, and J. E. Sipe, Phys. Rev. B **77**, 195202 (2008).

[13] S. Hallstein, J. D. Berger, M. Hilpert, H. C. Schneider, W. W. Rühle, F. Jahnke, S. W. Koch, H. M. Gibbs, G. Khitrova, and M. Oestreich, Phys. Rev. B **56**, R7076 (1997).

[14] J. Rudolph, D. Hägele, H. M. Gibbs, G. Khitrova, and M. Oestreich, Appl. Phys. Lett. **82**, 4516 (2003).

[15] I. Appelbaum, B. Huang, and D. J. Monsma, Nature (London) **447**, 295 (2007).

[16] B. T. Jonker, G. Kioseoglou, A. T. Hanbicki, C. H. Li, and P. E. Thompson, Nat. Phys. **3**, 542 (2007).

[17] A. M. Tyryshkin, S. A. Lyon, W. Jantsch, and F. Schäffler, Phys. Rev. Lett. **94**, 126802 (2005).

[18] W. Jantsch, H. Malissa, Z. Wilamowski, H. Lichtenberger, G. Chen, F. Schaffler, and G. Bauer, J. Supercond. Novel Magn. **18**, 145 (2005).

[19] L. Grenet, M. Jamet, P. Noé, V. Calvo, J.-M. Hartmann, L. E. Nistor, B. Rodmacq, S. Auffret, P. Warin, and Y. Samson, Appl. Phys. Lett. **94**, 032502 (2009).

[20] *Silicon Photonics*, edited by L. Pavesi and D. Lockwood (Springer-Verlag, Berlin, 2004).

[21] A. V. Efanov and M. V. Entin, Phys. Status Solidi B **118**, 63 (1983).

[22] J. Liu, X. Sun, D. Pan, X. Wang, L. C. Kimerling, T. L. Koch, and J. Michel, Opt. Express **15**, 11272 (2007).

[23] Y.-H. Kuo, Y. Lee, Y. Ge, S. Ren, J. Roth, T. Kamins, D. A. Miller, and J. Harris, Nature (London) **437**, 1334 (2005).

[24] M. Bonfanti, E. Grilli, M. Guzzi, M. Virgilio, G. Grosso, D. Chrastina, G. Isella, H. von Känel, and A. Neels, Phys. Rev. B **78**, 041407(R) (2008).

[25] X. Sun, J. Liu, L. C. Kimerling, and J. Michel, Opt. Lett. **34**, 1198 (2009).

[26] S.-W. Chang and S. L. Chuang, IEEE J. Quantum Electron. **43**, 249 (2007).

[27] K. Driscoll and R. Paiella, Appl. Phys. Lett. **89**, 191110 (2006).

[28] G. Sun, H. H. Cheng, J. Menéndez, J. B. Khurgin, and R. A. Soref, Appl. Phys. Lett. **90**, 251105 (2007).

[29] G. Capellini, M. De Seta, F. Evangelisti, V. A. Zinovyev, G. Vastola, F. Montalenti, and L. Miglio, Phys. Rev. Lett. **96**, 106102 (2006).

[30] B. D. Oskotskij, A. V. Subashiev, and Y. A. Mamaev, Phys. Low-Dimens. Semicond. Struct. **1/2**, 77 (1997).

[31] M. Agrawal and G. S. Solomon, Appl. Phys. Lett. **85**, 1820 (2004).

[32] G. Ciasca, M. De Seta, G. Capellini, F. Evangelisti, M. Ortolani, M. Virgilio, G. Grosso, A. Nucara, and P. Calvani, Phys. Rev. B **79**, 085302 (2009).

[33] M. Virgilio and G. Grosso, Phys. Rev. B **77**, 165315 (2008).

[34] C. G. Van de Walle and R. M. Martin, Phys. Rev. B **34**, 5621 (1986).

[35] M. Virgilio and G. Grosso, Phys. Rev. B **75**, 235428 (2007).

[36] J.-M. Jancu, R. Scholz, F. Beltram, and F. Bassani, Phys. Rev. B **57**, 6493 (1998).

[37] T. B. Boykin, N. Kharche, G. Klimeck, and M. Korkusinski, J. Phys.: Condens. Matter **19**, 036203 (2007).

[38] M. M. Rieger and P. Vogl, Phys. Rev. B **48**, 14276 (1993).

[39] H. Huang and S. Kock, *Quantum Theory of the Optical and Electronic Properties of Semiconductors* (World Scientific, Singapore, 1990).

[40] Y.-H. Kuo, Y. K. Lee, Y. Ge, S. Ren, J. E. Roth, T. I. Kamins, D. A. B. Miller, and J. S. Harris, Jr., IEEE J. Sel. Top. Quantum Electron. **12**, 1503 (2006).

[41] Y.-H. Kuo and Y.-S. Li, Phys. Rev. B **79**, 245328 (2009).

[42] Y.-H. Kuo and Y.-S. Li, Appl. Phys. Lett. **94**, 121101 (2009).

[43] A. Twardowski and C. Hermann, Phys. Rev. B **35**, 8144 (1987).

[44] M. O. Nestoklon, E. L. Ivchenko, J.-M. Jancu, and P. Voisin, Phys. Rev. B **77**, 155328 (2008).

[45] M. Virgilio, M. Bonfanti, D. Chrastina, A. Neels, G. Isella, E. Grilli, M. Guzzi, G. Grosso, H. Sigg, and H. von Känel, Phys. Rev. B **79**, 075323 (2009).